Paper No. 518

Third International Conference on Multiphase Flow, ICMF'98
Lyon, France, June 8-12, 1998

LES OF GAS-PARTICLE TURBULENT CHANNEL FLOW (THE EFFECT OF INTER-PARTICLE COLLISION ON STRUCTURE OF PARTICLE DISTRIBUTION)

Yamamoto, Y., Tanaka, T. and Tsuji, Y.
Department of Mechanical Engineering, Osaka University, Suita 565, JAPAN

Abstract

Particle dispersion in a fully-developed turbulent flow was studied. Numerical simulations with two-way coupling were performed for downward particle-laden turbulent flows in a vertical channel. Fluid turbulence was calculated by using LES, while the particle motion was treated by Lagrangean approach. In addition, inter-particle collision was taken into consideration. In this work, we focused our attention on the spatial structure of turbulence and particle distribution in the near-wall and the channel center regions. Furthermore, the effect of inter-particle collision on the spatial structure of particle distribution was discussed. It was found that the inter-particle collision affects the particle concentration distribution in the range of the present condition. The spatial structure and scale of clusters obtained by numerical simulation with inter-particle collision agree well with those of the experiments by Fessler et al. (1994)

Introduction

Interactions between particles and fluid turbulence, which are the turbulence modification in fluid flows and the effect of fluid turbulence on the particle motion, have been physically interesting phenomena in gas-particle flows. In this two decades the turbulence modification has been attracting many researchers attentions, and many studies have been conducted. There are some papers which intend to correlate the experimental data (for example, Gore & Crowe 1989), however the physics of the turbulence modification has not been clarified sufficiently.

In these days, some numerical simulations of two-phase turbulent flow have been performed by using the direct simulation techniques of turbulent flow (Squires & Eaton 1990, Elghobashi & Truesdell 1992). Regarding turbulent channel flows, Rouson & Eaton (1994) performed DNS and Wang & Squires (1996) performed LES. Both group showed that heavy particles tend to disperse uniformly and light particles form clusters.

The authors have performed LES of particle-laden turbulent channel flow (Tanaka et al. 1997) in the same conditions as the experiments by Kulick et al. (1993). We have compared the numerical results with their experimental ones and pointed out the effect of inter-particle collision is very large especially on the statistical properties of particle motion. In this paper, the instantaneous spatial structures of particle distribution and gas turbulence are studied. The correlation between them and the effect of inter-particle collision on the structure are discussed. Also, particle distribution obtained by numerical simulations are compared with the experiment by Fessler et al. (1994).

Numerical simulation

Particle motion

The algorithm of inter-particle collision is a key point in this work, because it greatly affects the computation time. We followed the technique of uncoupling developed by Bird (1976). By using this technique, the calculation of particle motion is split up into two stages. In the first stage, all particles are moved based on equation of motion free from particle-particle interaction. In the second stage, particle-wall and inter-particle collision are calculated. The occurrence of inter-particle collision during the first stage is examined for all particles. If a particle collides with another particle, then the velocities of collision pair are replaced by post-collision ones without changing their position. This technique of uncoupling requires that the time step in calculation must be much smaller than the mean free time, which is discussed later.

Particle Motion without Collision

The particle motion for a small rigid sphere in a turbulent flow field is described by a complicated integrodifferential equation (Maxey & Riley, 1983). However, if the density of the particle is substantially larger than the density of the carrier fluid, the equation of particle motion can be simplified. The equation of translational motion used in the simulations is given by,

$$m_p \frac{du_{pi}}{dt} = \frac{1}{2}\rho|\mathbf{u}_R|A\left[C_D u_{Ri} + C_{LR}\frac{(\mathbf{u}_R \times \omega_R)_i}{|\omega_R|}\right] + f_{LG}\delta_{i2} + m_p g\delta_{i1} \quad (1)$$

where m_p is particle mass, u_{pi} , particle velocity, C_D, drag coefficient, ρ, gas density, A, projected area of particle, C_{LR}, lift coefficient due to particle rotation, ω_{Ri}, particle rotational velocity, and u_{Ri} is gas velocity relative to the particle. The first term in the rhs of Eq.

(1) denotes the drag force, the second term, the lift force due to rotation, f_{LG}, the lift force due to velocity gradient and g is acceleration of gravity. The empirical relation for C_D by Schiller & Nauman (1933) was employed,

$$C_D = \frac{24}{\mathrm{Re}_p}\left(1 + 0.15\,\mathrm{Re}_p{}^{0.687}\right), \tag{2}$$

where Re_p is the particle Reynolds number, $\mathrm{Re}_p = d_p|\mathbf{u}_R|/\nu$ (d_p: particle diameter, ν: kinematic viscosity of gas). The lift coefficient C_{LR} was decided from the experimental data by Maccoll (1928). For the lift force f_{LG} was employed only in the wall-normal component with Saffman's expression as follows (1965),

$$f_{LG} = -1.62 d_p{}^2 \rho u_{Rx} \sqrt{\nu\left|\frac{\partial u_{Rx}}{\partial y}\right|}\,\frac{\partial u_{Rx}/\partial y}{|\partial u_{Rx}/\partial y|}. \tag{3}$$

The equation of rotational motion of a particle is given by,

$$I\frac{d\omega_{pi}}{dt} = -C_T\,\frac{1}{2}\rho\left(\frac{d_p}{2}\right)^2|\omega_R|\omega_{Ri}, \tag{4}$$

where I is the moment of inertia of a particle. The rhs of Eq. (4) is the viscous torque against the particle rotation, which is theoretically obtained by Dennis et al. (1980) and Takagi (1977). C_T is the non-dimensional coefficient determined by the rotational Reynolds number, $\mathrm{Re}_R = d_p{}^2|\boldsymbol{\omega}_R|/4\nu$.

The particle equation of motion is solved by using interpolated instantaneous fluid velocities at the particle position. 3-dimensional polynomial interpolation using values at eight grid-points surrounding the particle is applied. The particle velocity and rotational velocity are integrated by Eular method and the particle position by Crank-Nicolson scheme.

Collision

Particle concentration is assumed to be so low that binary collisions are overwhelming. Furthermore it is supposed that the period of collision is so small that only the impulsive force can contribute to change the momentum of particle in the period.

As the method examining whether inter-particle collision occurs, the stochastic one (Yonemura et al. 1993) or the deterministic one (Tanaka & Tsuji 1991) have been used. In this work, particle number density is so low that the statistical method cannot be used, so that we use the deterministic method. Outline of the procedure is as follows. Let us consider that a particle l collides with another particle m during one time step Δt_c. The particles are assumed to do linear motions with constant velocities during this time step. Fig. 1 shows the relative motion of particle l to m, where $\mathbf{r}_R\left(\equiv \mathbf{r}_m - \mathbf{r}_l\right)$, is the relative position vector. The relative distance between the two particles is given by $\left|\mathbf{r}_{R0} + k\left(\mathbf{r}_{R\Delta t} - \mathbf{r}_{R0}\right)\right|$, where k represents a non-dimensional time normalized by Δt_c. The condition required for the collision during this time step is that the following equation of k,

$$\left|\mathbf{r}_{R0} + k\left(\mathbf{r}_{R\Delta t} - \mathbf{r}_{R0}\right)\right|^2 = d_p^2 \tag{5}$$

has two real roots k_1 and k_2 $\left(k_1 < k_2, 0 \le k_1 < 1\right)$. The relative position vector of the collision is given by

$$\mathbf{r}_{Rc} = \mathbf{r}_{R0} + k_1\left(\mathbf{r}_{\Delta t} - \mathbf{r}_{R0}\right). \tag{6}$$

Inter-particle collision is examined by examining Eq. (5) for all neighboring particles.

The particle motion after the collision is described by the equation of impulsive motion:

$$\tilde{\mathbf{u}}_{pl} = \mathbf{u}_{pl} + \frac{\mathbf{J}}{m_p}, \tag{7}$$

$$\tilde{\mathbf{u}}_{pm} = \mathbf{u}_{pm} - \frac{\mathbf{J}}{m_p}, \tag{8}$$

$$\tilde{\boldsymbol{\omega}}_{pl} = \boldsymbol{\omega}_{pl} + \frac{d_p}{2I}\mathbf{n}\times\mathbf{J}, \tag{9}$$

$$\tilde{\boldsymbol{\omega}}_{pm} = \boldsymbol{\omega}_{pm} + \frac{d_p}{2I}\mathbf{n}\times\mathbf{J}. \tag{10}$$

$\mathbf{J}$ is the impulsive force exerted on particle l and $\mathbf{n}$ is the normal unit vector directed from the center of particle l to the contact point given by $\mathbf{n} = \mathbf{r}_{Rc}/|\mathbf{r}_{Rc}|$. Post-collision quantities are indicated by a tilde. Assuming spherical particles, a constant coefficient of restitution e and negligible particle deformation, $\mathbf{J}$ is given by (Tanaka & Tsuji, 1991):

$$\mathbf{J} = J_n\mathbf{n} + J_t\mathbf{t}, \tag{11}$$

$$J_n = (1+e)M\mathbf{c}\cdot\mathbf{n}, \tag{12}$$

$$J_t = \min\left[-\mu_f J_n, \frac{2}{7}M|\mathbf{c}_{fc}|\right]. \tag{13}$$

In the above equations, $\mathbf{t}$ is the tangential unit vector directed to the slip velocity of particle m to l, e is the coefficient of restitution, μ_f is the coefficient of friction and $M=m_p/2$ for inter-particle collision and $M=m_p$ for particle-wall collision. $\mathbf{c}$ is the relative velocity of mass center, $\mathbf{c} = \mathbf{u}_{pm} - \mathbf{u}_{pl}$, and $\mathbf{c}_{fc}$ is the slip velocity at the contact point given by,

$$\mathbf{c}_{fc} = \mathbf{c} - (\mathbf{c}\cdot\mathbf{n})\mathbf{n} - \frac{d_p}{2}\boldsymbol{\omega}_{pl}\times\mathbf{n} - \frac{d_p}{2}\boldsymbol{\omega}_{pm}\times\mathbf{n}.$$

For inter-particle collision, the velocities and rotational velocities are replaced by equation (7)-(10). For particle-wall collision, the time interval Δt is subdivided into Δt_w and $\Delta t - \Delta t_w$. Δt_w is the time before the collision. Each particle is moved in Δt_w by using the pre-collision quantities, and in $\Delta t - \Delta t_w$ by using the post-collision ones.

Fluid motion

To get the fluid flow field, large eddy simulation (LES) is applied. In LES fluid flow is divided into large scale motion and small scale fluctuation, so called sub-grid scale (SGS) fluctuation, by ®filtering©. Large scale flow is calculated directly with model of the effect of SGS fluctuation.

The filtered equations of continuity and momentum are as follows.

$$\frac{\partial u_i}{\partial x_i} = 0, \tag{14}$$

$$\left.\begin{aligned} \frac{\partial u_i}{\partial t} &= \frac{\partial F_{ij}}{\partial x_j} + \frac{F_{pi}}{\rho} \\ F_{ij} &= -\delta_{ij}\frac{p}{\rho} - u_i u_j + 2\nu S_{ij} - \overline{u'_i u'_j}^{(SGS)} \end{aligned}\right\}, \tag{15}$$

where u_i and p are grid scale velocity and pressure. F_{pi} is the reaction of fluid force on particles contained in a unit mass of fluid element. In this study, solid volume fraction is so low that the volume of particle is neglected in the fluid calculation. S_{ij} is strain rate tensor, $S_{ij} = (1/2)\left(\partial u_i/\partial x_j + \partial u_j/\partial x_i\right)$ and $\overline{u'_i u'_j}^{(SGS)}$ is SGS Reynolds stress. In this work, we neglected the effect of particles on SGS stress because of lack of idea of modification due to the presence of coarse particles. Therefore the following model which is preferred for single phase turbulent channel flows was used. As SGS model, we applied Smagorinsky model (Deardorff, 1970),

$$\left.\begin{aligned} \overline{u'_i u'_j}^{(SGS)} &= 2\nu_{SGS}S_{ij} - \frac{1}{3}\delta_{ij}\overline{u'_k u'_k}^{(SGS)} \\ \nu_{SGS} &= \left(C_s f_s \Delta_s\right)^2 \sqrt{2S_{ij}S_{ij}} \end{aligned}\right\}, \tag{16}$$

where Smagorinsky constant C_s=0.1, filter scale $\Delta_s = \sqrt[3]{\Delta x \Delta y \Delta z}$, and f_s is damping function, $f_s = 1 - \exp\left(-y^+/25\right)$. Using these models, F_{ij} in Eq. (15) is modified as follows,

$$\left.\begin{aligned} F_{ij} &= -\delta_{ij}P - u_i u_j + 2\left(\nu + \nu_{SGS}\right)S_{ij} \\ P &= \frac{p}{\rho} + \frac{1}{3}\overline{u'_k u'_k}^{(SGS)} \end{aligned}\right\}. \tag{17}$$

These equations were solved by finite difference method. Spatial derivatives were approximated by second-order accuracy central finite difference on staggered grids. Non-linear term and viscous term were treated explicitly, and pressure term and equation of continuity were treated implicitly. Second-order Adams-Bashforth method was applied for time marching Poisson equation for pressure was solved using Fourier series expansions in the streamwise and spanwise directions together with tridiagonal matrix inversion.

Simulation condition

The simulations are performed under the same conditions as chosen in the experiments by Kulick et al. (1993), and Fessler et al. (1994). The channel width is H=0.04 [m], the length of the calculation region in streamwise direction H_x=2.2H and in spanwise direction is H_z=0.74H. The calculation region is shown in Fig. 2. We chose gas as fluid and its kinematic viscosity as ν=1.5×10^{-5}[m^2/s], and mean friction velocity as u_τ=0.49[m/s]. Reynolds number based on channel width and friction velocity is 1300. In homogeneous direction (*i.e.* streamwise and spanwise), periodical boundary condition is applied. The flow is driven by constant pressure gradient. The simulation is performed using 64×48×64 grid points in x, y, and z direction. Uniform grids were applied in the streamwise and spanwise directions. In the wall-normal direction, grid points were concentrated in the near-wall region using hyperbolic function. The grid spacing given in wall units are Dx^+=45, Dz^+=15, Dy^+_{min}=2.8 beside to the wall and Dy^+_{max}=63.3 at the channel center. We have found out this resolution is high enough to calculate the particle motion precisely (Yamamoto et al. 1998).

Conditions of particle are shown in Table 1. We choose the coefficient of restitution as e=0.95 and the coefficient of friction as μ

The time step for calculation of fluid motion and for particle motion free from collision is Δt=8.2×10^{-6} [sec] and the time step for calculation of inter-particle collision is Δt_c=5Δt. This is much smaller than the particle relaxation time τ_p, so that inter-particle collisions are examined assuming particles motion is linear during Δt_c. In case that the technique of uncoupling is used, the time step for collision calculation Δt_c should be much smaller than the mean free time τ_l. We estimate τ_l by,

$$\tau_l = 1\left(\sqrt{2}\pi d_p^2 n \sqrt{\overline{u'^2_p}}\right)$$

where n is the particle number density. Estimated value of $\Delta t_c/\tau_l$ is $O(10^{-3})$, so Δt_c used in our simulation is found to be suitable.

Initial condition for particles is as follows. Particles are distributed uniformly in the calculation region by random numbers and the velocities of particles are set equal to the fluid velocities at the particle position. In order to study the effect of inter-particle collision, both the cases with and without inter-particle collision are calculated in all conditions.

All the calculation were executed on the NEC SX-4 at Osaka University Computation Center. A simulation for the lycopodium particles considering inter-particle collision took about 20 CPU hours.

Results

Near-wall region

Fig. 3 shows the instantaneous distribution of the copper particles in the wall-parallel plane in the near-wall region (y^+: 0~65). Fig. 4 shows the instantaneous distribution of gas streamwise fluctuation velocity at y^+=4 at the same instance as Fig.3 (lighter region : high speed, darker region : low speed). The copper particles, which have large inertia, show nearly uniform distribution regardless of inter-particle collision. They show large inertia particle cannot be affected by the streaky structure of gas turbulence.

Fig. 5 shows the instantaneous distribution of the glass particles (y^+: 0~4) and Fig. 6 shows the streamwise fluctuation velocity distribution at y^+=4. Fig. 6 shows the streaky structure clearly.

Comparing Fig. 5(a) and 6(a), particle concentration is high in low-speed regions and this result shows the same tendency as those by Rouson & Eaton (1994) and Wang & Squires (1996). This kind of particle concentration is referred as the preferential concentration. This agreement is reasonable because they also neglected the inter-particle collision and assumed one-way coupling. This phenomenon is caused by the effect of quasi-streamwise vortex. Particles are transported to the near-wall region by sweep and accumulated in ejection regions, and then kept close to the wall by shear-induced lift force.

In the cases of two-way coupling without inter-particle collision shown in Fig. 5(b) and 6(b), particle concentration is high in high-speed regions in contrast with the case of one-way coupling. This is because the large downward force acting on the fluid in dense regions due to gravity on particles. In the present calculation condition gas flows downward so that the direction of gravity on particles coincides with the flow direction. Consequently gas in dense region is dragged more strongly by particles through the reaction of fluid drug than in dilute region.

In the case of two-way coupling with inter-particle collision shown in Fig 5(c) and 6(c), streaky structure of particle distribution cannot be observed. Particle concentration in the near-wall region is low because the inter-particle collision disperses particles in the wall-normal direction.

Fig. 7 shows the instantaneous distribution of the lycopodium particles in the near-wall region (y^+: 0~4) and Fig. 8 shows the streamwise fluctuation velocity distribution at y^+=4 corresponding to Fig. 7. In the case of one-way coupling without inter-particle collision shown in Fig. 7(a) and 8(a), particles tend to concentrate to low-speed regions. This tendency is same as the glass particles, but is more stronger and scale of clusters is smaller than that of glass particles. In the case of two-way coupling with inter-particle collision shown in Fig 7(b) and 8(b), particles are distributed nearly uniformly because inter-particle collision diffuses the particle clusters. In addition to these cases we tried to calculate the case of two-way coupling without inter-particle collision but calculation cannot be executed well because of extreme accumulation of particles in the near-wall region.

Channel center

Fig. 9 Fig 10 and Fig 11 show the instantaneous distributions of the copper particles, the glass particles and the lycopodium particles respectively in the wall-parallel plane in the channel-center region (sheet thickness : 2[mm]). Large-inertia particles tend to disperse uniformly and small-inertia particles tend to form the preferential concentration or particle clusters. It is found that the smaller the inertia of particles the smaller the cluster size. In the case of neglecting inter-particle collision, small-inertia particles tend to accumulate in the near-wall region and especially the concentration of lycopodium particles is very low in the channel-center region. In an LES by Wang & Squires (1996) of same Reynolds number as the present one, such extreme accumulation did not occur because they neglected the lift force due to velocity gradient.

Fessler et al. (1994) made an experiment corresponding to the present condition and measured the particle distribution in the channel-center region. The present result of particle concentration considering inter-particle collision expresses well the tendency of the experiment. The experiment shows that clusters of lycopodium particles tend to be long in the spanwise direction and short in the streamwise direction. The LES by Wang & Squires (1996) predicted clusters long in the streamwise direction similar to those in the near-wall region. The characteristics of clusters predicted in the present simulation agrees well in scale and structure with the experiment.

Conclusions

An LES of gas-solid turbulent channel flow with two-way coupling considering inter-particle collision was performed in the same conditions as those of the experiments by Fessler et al. (1994). The principal results are as follows.

(1) Large-inertia particles tend to disperse uniformly and small-inertia particles tend to form the preferential concentration or particle clusters, and this tendency agrees well with the previous experiments or numerical simulations.

(2) Both of two-way coupling and inter-particle collision largely affect the particle concentration both in the near-wall and the channel-center regions. In the near-wall region, the one-way and no-collision simulation predicted that particles concentrate to low-speed streaks, while the two-way and no-collision simulation predicted the opposite correlation. Furthermore, the simulation considering both effects predicted uniform particle distributions in the near-wall region.

(3) In the channel-center region, the scale and shape of clusters predicted by the present numerical simulation considering inter-particle collision is in good agreement with experiment by Fessler et al. (1994).

References

Deardorff, J.W., A numerical study of three-dimensional turbulent channel flow at large Reynolds number, *J. Fluid Mech.* **41**(2), (1970), 453-480.

Dennis, S. C. R., Singh, S. N. & Ingham, D. B., The steady flow due to a rotating sphere at low and moderate Reynolds numbers, *J. Fluid Mech.*, **101**, (1980), 257-279.

Elghobashi, S. & Truesdell, G. C., Direct simulation of particle dispersion in a decaying isotropic turbulence., *J. Fluid Mech.*, **242**, (1992), 655-700.

Fessler, J. R., Kulick, J. D. & Eaton, J. K., Preferential concentration of heavy particles in a turbulent channel flow., *Phys. Fluids*, **6**(11), (1994), 3742-3749.

Gore, R. A. & Crowe, C. T., Effect of particle size on modulating turbulent intensity: Influence of radial location. *ASME/FED Turbulence Modifications in Dispersed Multiphase Flows*, (ed. E.E. Michaelides & D.E. Stock), **80**, (1989), 31-35.

Kulick, J. D., Fessler, J. R. & Eaton, J. K., Particle response and turbulence modification in fully developed channel flow., *J. Fluid Mech.*, **277**, (1994), 109-134.

Maccoll, J. H., Aerodynamics of a spinning sphere., *J. Roy. Aero Sci.*, **32**, (1928), 777-798.

Maxey, M. R. & Riley, J. J., Equation of motion for a small rigid sphere in nonuniform flow., *Phys. Fluids*, **26**, (1983), 883-889.

Pedinotti

Rouson, D. W. I. & Eaton, J. K., Direct numerical simulation of turbulent channel flow with immersed particles., *ASME/FED Numerical Methods in Multiphase Flows* (ed. Sommerfeld, M.), **185**, (1994).

Saffman, P. G., The lift on a small sphere in a slow shear flow., *J. Fluid Mech.*, **22**, (1965), 385-400.

Schiller, L. & Nauman, A., *V. D. I. Zeits*, **77** (1933), 318.

Squires, D. K. & Eaton, J. K., Particle response and turbulence modification in isotropic turbulence., *Phys. Fluids*, A**2** (7), (1990), 1191-1203.

Takagi, H., Viscous flow induced by slow rotation of a sphere, *J. Phys. Soc. Japan*, 42, (1977), 319-325.

Tanaka, T. & Tsuji, Y., Numerical Simulation of Gas-Solid Two-Phase Flow in a Vertical Pipe: On the Effect of Inter-Particle Collision, *ASME/FED Gas-Solid Flows*, (1991), 123-128.

Tanaka, T., Yamamoto, Y. Potthoff, M. & Tsuji, T., LES of gas-particle turbulent channel flow, *Proceedings of the ASME Fluids Engineering Division Summer Meeting*, (1997), FEDSM97-3630(CD-ROM).

Wang, Q. & Squires, K. D., Large eddy simulation of particle-laden turbulent channel flow., *Phys. Fluids*, **8**(5), (1996), 1207-1223.

Yamamoto, Y., Tanaka, T. & Tsuji, T., Effect of spatial resolution of LES on particle motion, *Proceedings of the ASME/FED 3rd Int. Symp. Numerical Methods in Multiphase Flows*, to be presented, (1998).

Yonemura, S., Tanaka, T. and Tsuji, Y., Cluster formation in gas-solid flow predicted by the DSMC method, *ASME/FED Gas-Solid Flows*, (1993), 303-309.

Table 1: Particle parameters

Material	Lycopodium	Glass	Copper
Density ρ_p [kg/m^3]	700	2500	8800
Diameter d_p [μm]	28	50	70
Stokes relaxation time τ_p [ms]	1.7	19	133
Terminal velocity v_t [m/s]	0.016	0.18	0.93
$St = \tau_p / (H/u_\tau)$	0.021	0.23	1.6
$St^+ = \tau_p / (\nu/u_\tau^2)$	27	301	2110
Mass loading ratio ϕ	0.01	0.2	1
Number of particle	156159	154214	79445

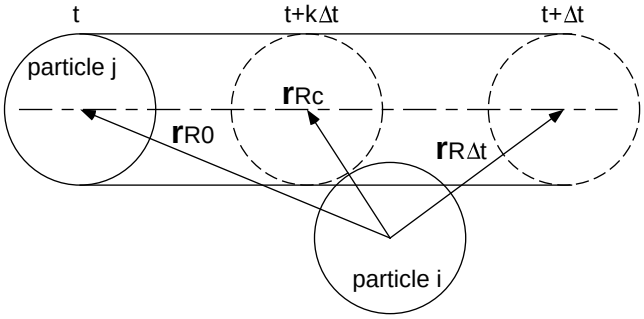

Figure 1: Inter-particle collision

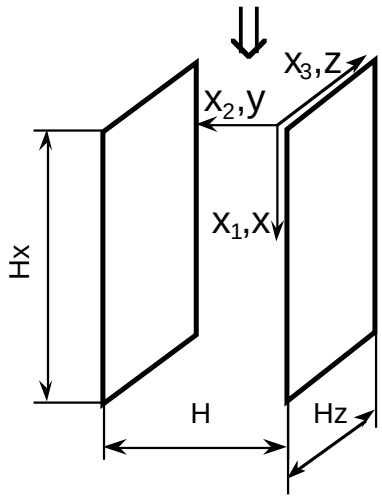

Figure 2: Calculation region

(a) 2-way without collision

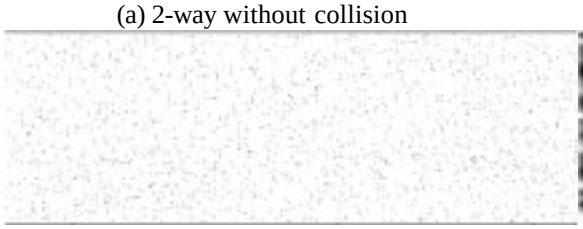

(b) 2-way with collision

Figure 3: Particle distribution on wall-parallel plane in the-wall region, copper particle (y: 0~2[mm], y^+: 0~65)

(a) 2-way without collision

(b) 2-way with collision

Figure 4: Streamwise fluctuation velocity on wall-parallel plane in the-wall region (y=0.1[mm], y^+=4, lighter region: high speed, darker region: low speed)

(a) 1-way without collision

(b) 2-way without collision

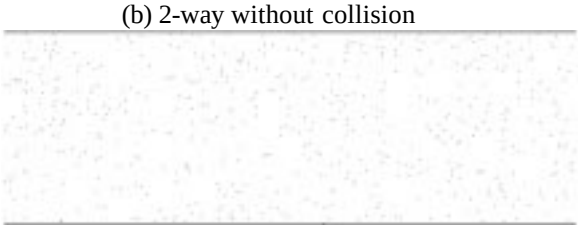

(c) 2-way with collision

Figure 5: Particle distribution on wall-parallel plane in the-wall region, glass particle(y: 0~0.1[mm], y^+: 0~4)

(a) 1-way without collision

(b) 2-way without collision

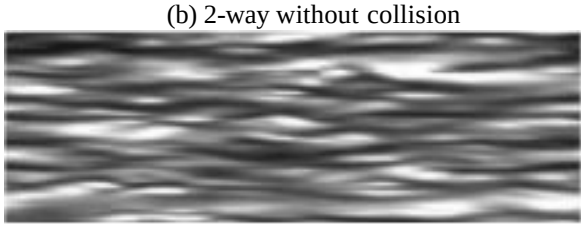

(c) 2-way with collision

Figure 6: Streamwise fluctuation velocity on wall-parallel plane in the-wall region (y=0.1[mm], y^+=4)

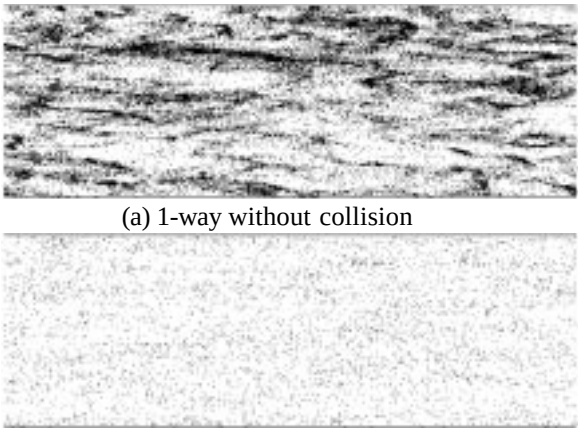

(a) 1-way without collision

(b) 2-way with collision

Figure 7: Particle distribution on wall-parallel plane in the-wall region, lycopodium particle(y^+: 0~4)

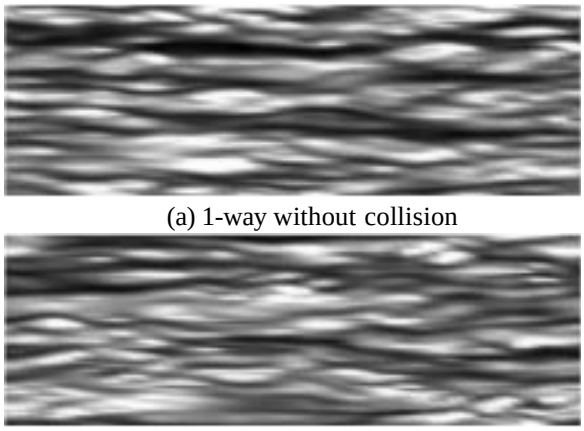

(a) 1-way without collision

(b) 2-way with collision

Figure 8: Streamwise fluctuation velocity on wall-parallel plane in the-wall region (y=0.1[mm], y^+=4)

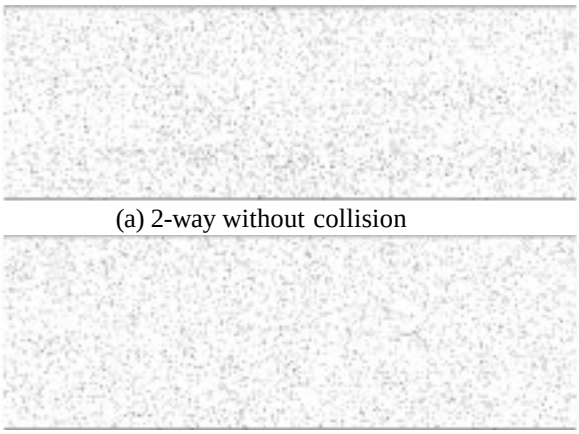

(a) 2-way without collision

(b) 2-way with collision

Figure 9: Particle distribution on wall-parallel plane in the channel-center region, copper particle (thickness=2[mm])

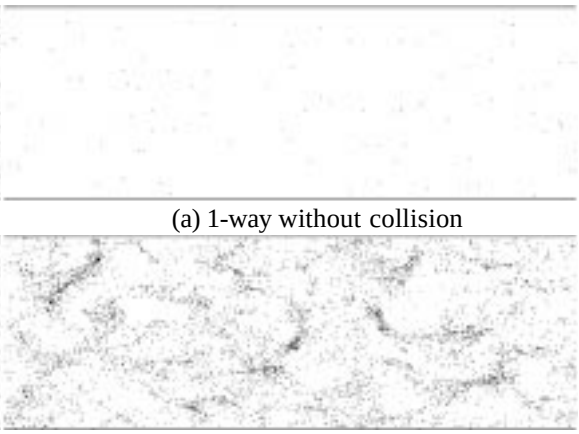

(a) 1-way without collision

(b) 2-way with collision

Figure 11: Particle distribution on wall-parallel plane in the channel-center region , lycopodium particle

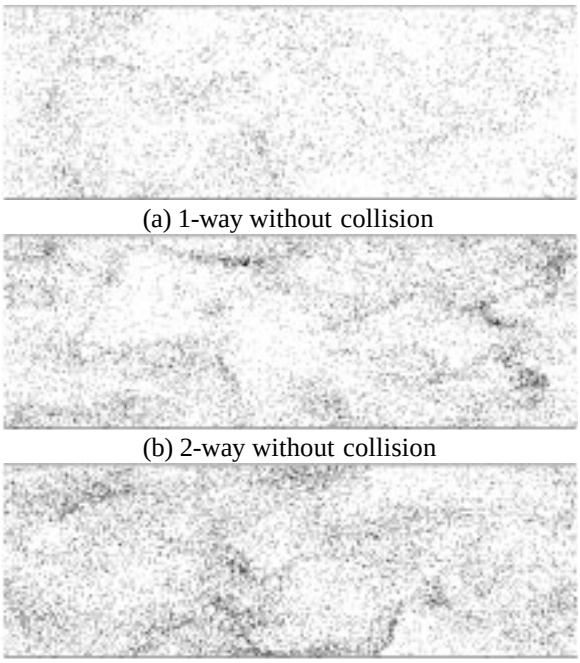

(a) 1-way without collision

(b) 2-way without collision

(c) 2-way with collision

Figure 10: Particle distribution on wall-parallel plane in the channel-center region, glass particle